Civil Engineering Infrastructures Journal xx,xx
DOI: 10.22059/ceij.2024.372952.2018

Optimizing the performance of L-shaped concrete-filled steel tube columns under eccentric loading

Mojtaba Labibzadeh[1], *Mostafa Kordi, Abbas Rezaeian, Farhad Hosseinlou, Majid Khayat*

Faculty of Civil Engineering and Architecture, Shahid Chamran University of Ahvaz, Ahvaz, Iran

Received: 21/02/2024
Revised: 05/04/2024
Accepted: 21/04/2024

ABSTRACT

Special-shaped concrete-filled steel tube (SCFST) columns have a higher bearing capacity, ductility, and energy absorption compared to other columns. Due to their special shape, the columns can be utilized in different parts of the building without protruding members. In L-shaped CFST columns, this study investigated the effect of various parameters (such as yield stress of steel wall, characteristic strength of concrete, height of column, thickness of steel wall, and geometry of stiffeners) on the eccentric load bearing capacity. In other words, the bearing capacity has been measured based on the optimal performance of these columns under the effect of axial and eccentric loads. The results of this study showed that the bearing capacity of L-shaped CFST columns is highly dependent on all the parameters mentioned above and that the column's optimal performance can be determined by carefully selecting and optimizing these parameters. Also, the ratio of load-to-weight (P/W) has been considered. Load-displacement diagrams and the weight of steels used in different columns are compared. Based on the obtained results, the changing of the thickness and strength of the steel wall has a significant effect on increasing the bearing capacity. Whereas, the concrete strength has a lesser effect on the bearing capacity of the columns. The columns with greater thickness perform better than the columns with less thickness in terms of ductility and energy absorption capacity under eccentric loading.

Keyword:

Special-shaped column
Concrete-filled steel tube column
Eccentric bearing capacity
Optimal performance

1. Introduction

[1] Corresponding author: labibzadeh_m@scu.ac.ir

Special-shaped concrete-filled steel tube (SCFST) columns have lower steel consumption ratio and more stiffness than normal steel columns, and this is due to the presence of concrete inside the steel pipe. Also, in a reinforced concrete column, only transverse reinforcements create confinement pressure for the concrete core, while in the steel column filled with concrete, the entire steel wall plays the role of confinement for the concrete core. In buildings, columns with a special shape do not occupy much space, and as a result, they are generally useful in terms of architecture. There is no cost of column formatting when using the concrete-filled steel tube columns (Hatzigeorgiou and Beskos, 2004; Dundar et al., 2008). Despite all the advantages of SCFST columns, the use of these columns has limitations. The complexity of connecting beams to these columns and the lack of experience in construction are the most important limitations. Also, when the steel wall yields, the pressure on the concrete core increases greatly. Therefore, studying the behavior of SCFST columns under axial loading requires extensive studies (Ghandi et al. (2024)- Zhou et al. (2024)).

Chen et al. (2009) used laboratory tests to investigate the mechanical properties and failure processes of SCFST columns under compressive loads. In order to compare the final load capacities and failure modes from their simulations with the experimental observations, they also carried out finite element analysis. They also created methods to forecast these SCFST columns' compressive strength.

In 2019, Zhang et al. investigated the behavior of seven SCFST columns featuring double plate connections subjected to axial compressive forces. Their study assessed how variations in the height and width of these connecting plates affected column performance and led to the formulation of equations for calculating the columns' load-bearing capacity. The tests demonstrated that the double LCFST columns exhibited strong axial compressive performance and that the single columns performed effectively within the double LCFST column’s structural framework. They also utilized 3D nonlinear finite element models to analyze the mechanical properties and axial compressive behavior of the double LCFST columns, finding that the model results were consistent with the experimental data. Their parametric studies, based on these models, explored the impact of factors such as the thickness and width of vertical steel plates, the slenderness ratio, and the size and thickness of the steel pipe, and they proposed a new method for calculating the slenderness ratio.

Chen et al. conducted five sets of eccentric compression tests in a different study from 2021 to look at the mechanical characteristics of SCFST columns under axial stresses and bending moments around the center of mass's main axis. Their work, which followed international standards and integrated finite element calculations and experimental testing, produced a formula for evaluating the in-plane stability of SCFST columns that were bent and subjected to axial forces around the main axis.

Chen et al. (2021) investigated the effects of uniaxial eccentric compression on CFST composite columns with double sheet connections, taking into account varying eccentricities and loading directions. Axial load-displacement curves and fracture models from experimental testing as well as finite element calculations were compared. They proposed a new formula for the stability capacity of CFST composite columns with double plate connections and introduced a theoretical formula for predicting the bearing capacity of specimens under uniaxial eccentric compression. They did this by using the superposition principle and slenderness ratio calculation methods based on steel structure design standards.

The temperature distribution, axial deformation, fire resistance, and failure modes of LCFST columns were investigated by Yang et al. in 2022. Their parametric research showed that fire resistance is highly dependent on factors such component thickness, eccentricity ratio, slenderness ratio, and thickness of the fire protection layer. In comparison to the current CFST column fire design standards, they found that a thicker fire protection layer could result in higher fire resistance ratings for LCFST columns. They

also proposed simplified formulas for determining fire resistance and the required thickness of the fire protection layer, which could result in a 50% reduction in thickness.

Liu et al. (2024) investigated a novel L-shaped irregular concrete-filled steel tube column design, which offers enhanced convenience for installation and construction. Their study included tests on two full-scale specimens under axial compression and two under eccentric compression, and they developed finite element models to simulate the loading process. The results from the FE models were in close agreement with the experimental findings. Ma et al. (2024) studied L-shaped columns constructed from recycled aggregate concrete-filled steel tubes using eccentric compression tests and numerical validation, developing an N-M relationship curve for improved safety predictions. Chen et al. (2024) designed and tested a steel cage featuring transverse steel bars for ultra-thin high-strength steel tube high-strength concrete medium-long column specimens. Their findings showed that the steel cage effectively mitigated bulging in the specimens and enhanced the steel pipe's restraint on the concrete.

A review of existing research highlights ongoing limitations in understanding the behavior of CFST columns with specific shapes under eccentric loading conditions. This manuscript addresses these gaps by employing finite element modeling to study SCFST columns and exploring methods to improve their performance under eccentric loading scenarios. For the first time, this study considers the load-to-weight (P/W) ratio as a key factor for optimizing SCFST column performance under eccentric loading, aiming to identify the most effective columns based on their P/W ratios. The study evaluates a wide range of samples and distinguishes between the five best-performing and five weakest-performing columns across two categories: short and long columns.

2. Numerical Simulation

In fact, the SCFST columns are a special form of CFST columns that are made up of several single columns connected by sheets and stiffeners. These columns are divided into different types based on the shape of the cross-section and the placement of single columns and their connections. Some examples of these columns are shown in Figure 1.

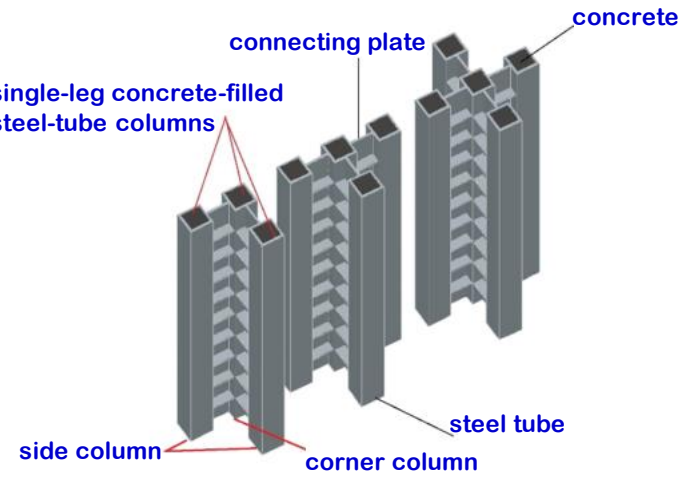

Figure 1: Different configurations of SCFST columns (Chen et al., 2020)

In this study, the simulation of SCFST columns is conducted using the finite element software ABAQUS. The numerical simulation process involves several key steps: modeling the column geometry, simulating the material behavior, defining boundary conditions and interactions between

model components, selecting appropriate element types and creating a mesh, applying the specified loading conditions to the model, and choosing the suitable analysis type.

2.1. *The geometry and Materials*

The SCFST column consists of several components, including a square steel tube, connecting plates, concrete, transverse stiffeners, loading plates, and both upper and lower column stiffeners as illustrated in Figure 2. In the ABAQUS software, these components are modeled separately. Each component is represented using C3D8R solid elements, which have three degrees of freedom. The modeling process involves first constructing the steel column and stiffeners, then filling the space with concrete, and finally placing the loading plate on top of the column to apply the force (Chen et al., 2024; Wang, 2024). To simulate the SCFST columns, both concrete and steel materials are utilized. The Concrete Damage Plasticity (CDP) model from the ABAQUS material library is employed to define the concrete's behavior. This model is based on two primary mechanisms for concrete failure: tensile cracking and compressive crushing (Labibzadeh et al., 2018; 2017).

The CDP model is capable of capturing the complex behavior of concrete through isotropic elastic damage coupled with plasticity for both compressive and tensile forces. It is also designed to handle dynamic, one-way, and cyclic loading conditions (Labibzadeh and Hamidi, 2017). The majority of credible research studies use the CDP model for concrete. For defining the elastic properties of concrete, the modulus of elasticity and Poisson's ratio are required, which can be obtained from laboratory tests or estimated using the American Concrete Institute (ACI 318, 2011) standards.

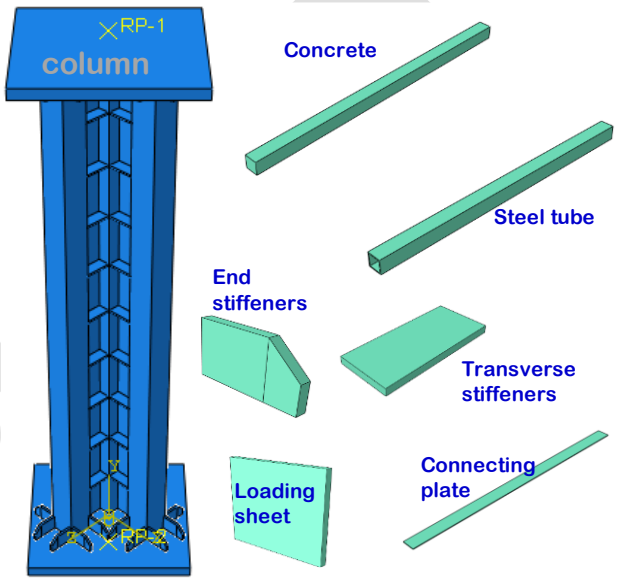

Figure 2: The column and its components modeled in ABAQUS

3. Results

3.1. *Eccentric bearing capacity of SCFST columns*

To investigate the effect of different parameters on the eccentric bearing capacity of SCFST columns, the different models with different specifications are built. For this purpose, all the investigated parameters are considered fixed (L0, C20, F250, H2, A25) and only one of them is changed. Then, the column is subjected to eccentric loading.

3.1.1. *Effect of steel tube thickness*

To compare energy absorption and ductility of SCFST columns under eccentric load, three specimens with thicknesses of 4, 6, and 8 mm have been considered. In the specimens simulated in ABAQUS, the specifications of examined columns are considered constant (C20, F250, H2000, A25) and only the thickness of the steel tube has changed (t=4, 6, and 8 mm). The dimensions of the steel tube are 100 (mm). Energy is equal to the area under the load-displacement diagram up to the peak point of the curve. In Figure 3, the bearing capacity of columns with different thicknesses and eccentric loading are compared. In Table 1, the amount of energy absorption of each column under eccentric loading is also listed. It can be seen that the amount of energy absorption of the column with tube thickness of 8 mm under loading with eccentricity of -120 mm is about 3.7 times more than the column with tube thickness of 4 mm and 1.7 times more than the column with tube thickness of 6 mm. Also, the energy absorption of the column with thickness of 8 mm under loading with eccentricity of 120 mm is 2.5 times more than the column with thickness of 4 mm and 1.5 times more than the column with thickness of 6 mm.

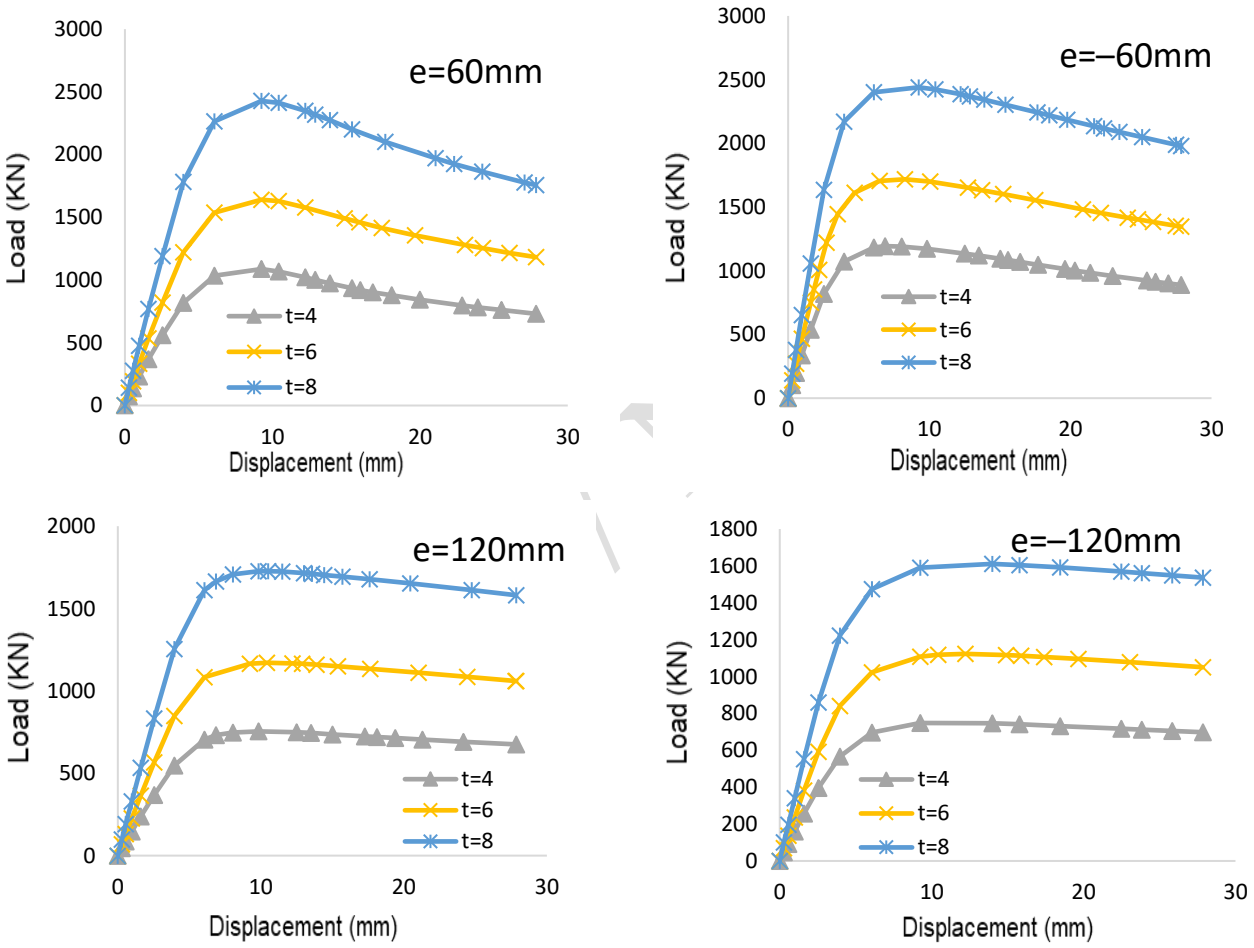

Figure 3: effect of steel tube thickness on load carrying capacity under eccentric loading

Table 1: Comparison of energy absorption of SCFST columns

Feature	E (kN.mm)	E (kN.mm)	E (kN.mm)	E (kN.mm)
Eccentricity (mm)	e=60	e=–60	e=120	e=–120
t=4 mm	4822.198	5234.006	5732.06	7035.35
t=6 mm	10457.41	8734.964	10601.38	10468.35
t=8 mm	17910.99	13100.36	17315.1	15359.85

The ductility of a member is the ability to deform plastic without the significant loss of strength before failure. Deformation capacity is generally utilized to acquire ductility. The ductility of the column is

calculated considering the P-Δ diagram. Relationship (3) is applied to calculate the ductility of columns (Tao et al., 2008; Dancygier and Berkover, 2016):

$$\mu_{0.85} = \frac{\Delta_{0.85}}{\Delta_y} \quad (3)$$

In this regard, $\Delta_{0.85}$ is the displacement corresponding to the point where capacity degrades to 85% of its peak. According to Figure 3 and Table 1, it can be stated that the eccentric bearing capacity of column with tube thickness of 8 mm under loading with e= −120 mm is about 1.4 times more than the bearing capacity of column with tube thickness of 6 mm and 2.15 times more than the column with tube thickness of 4 mm. Meanwhile, the weight of steel used in the column with tube thickness of 8 mm is 1.09 and 1.2 times more than the weight of steel used in the column with tube thickness of 6 mm and 4 mm, respectively. Also, the ductility of examined columns with the tube thickness of 8 mm under loading with e= −120 mm is 1.02 and 1.05 times that of the column with tube thickness of 6 mm and 4 mm, respectively Table 2.

Table 2: Comparison of energy absorption of

Feature	Pu (kN)	Pu (kN)	Pu (kN)	Pu (kN)	$\mu_{0.85}$	$\mu_{0.85}$	$\mu_{0.85}$	$\mu_{0.85}$
Eccentricity (mm)	e=60	e=−60	e=120	e=−120	e=60	e=−60	e=120	e=−120
t=4 mm	1088	1193	1635	748	3.18	5.3	6.04	8.4
t=6 mm	1640	1718	2342	1123	3.42	5.59	6.48	8.6
t=8 mm	2427	2420	2872	1610	3.65	6.48	6.95	8.8

3.1.2 *Columns with different eccentricities*

According to the outputs, it is clear that the best performance is for the specimen without eccentricity and the lowest height. Accordingly, in this sub-section, the effects of eccentricity are studied only on the short columns (H=2 m). Figure 4 presents the load-displacement curves for a column with a height of 2 meters subjected to various levels of eccentricity. The results demonstrate that eccentricity has a considerable effect on the column's load-bearing capacity. As eccentricity increases from 0 to 60 mm, the column's capacity drops by 95%, whereas increasing eccentricity from 0 to -60 mm leads to a 99% reduction in capacity. Furthermore, when eccentricity is increased to 120 mm and -120 mm, there is a 181% and 207% decrease in capacity, respectively. The column exhibits its poorest performance under the conditions of maximum height and the greatest negative eccentricity.

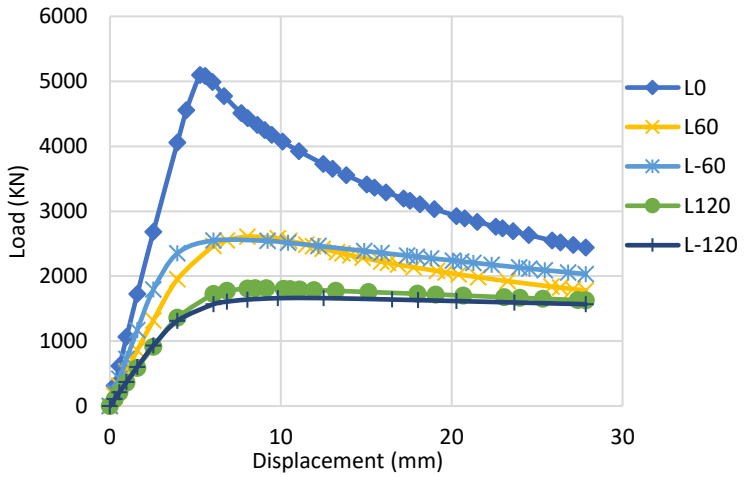

Figure 4: Load-displacement curve of column (H=2m) with different eccentricities

3.2. *Performance of the columns based on the* $\frac{P}{W}$ *index*

In this study, the numerical models simulated in ABAQUS have five different eccentricities (L= 0, 60, -60, 120, -120 mm), three types of concrete resistance (C=15, 20, 40 MPa), two types of steel tubes (F= 250, 400 MPa), three types of steel wall thickness (T= 4, 6, 8 mm), five types of height (H= 2, 3, 4, 5, 6 meters). Moreover, there are three types of columns with the stiffeners at different intervals (A= 20, 25, 35 mm). Also, due to the fact that the distance between the stiffeners has no effect on the bearing capacity of the column, a distance of 25 mm has been applied in all the models. According to the change of material and dimensions of each specimen, a total of 1100 model are evaluated. The load-to-weight ($\frac{P}{W}$) ratio is used to seek the best performance. In other words, the optimal column is the one that has the highest ratio of load-to-weight. To compare the overall performance of the columns, the specimens are divided into two types of short and long columns. Then, each of the short and long columns is examined separately, and the performance of each is studied according to the load-to-weight ratio.

In Table 3, the best and weakest performance of considered columns are summarized. In the last column of Table 3, the failure behavior of each specimen is referred. In this regard, the behavior of the column in the state of failure is revealed in Figures 5 to 7. In each figure, three points "A", "B" and "C" are specified along with von-Mises yield criterion. Point "A" is related to the yield stress of the column, point "B" is related to the maximum bearing capacity of the column, and point "C" represents the column's ductility. Also, P_u is the ultimate load, Δ_u is the ultimate displacement, P_y is the yield load, and Δ_y is the yield displacement. It is worth noting that $\mu_{0.85}$ indicates the ductility of the column. Based on the results, it is interesting that the specimen (column) with better performance based on the $\frac{P}{W}$ index has less ductility than the specimen with lower performance. Also, the specimen with better performance based on the $\frac{P}{W}$ index has the highest carrying capacity.

Table 3: Short columns with the Best and weakest performance based on the $\frac{P}{W}$ index

performance	Height (m)	Wall thickness (mm)	Yield stress of steel (MPa)	Compressive strength of concrete (MPa)	Eccentricity (mm)	$(\frac{P}{W})$	behavior
best	2	8	400	40	0	1.34	Figure 11
weakest	4	4	250	15	-120	0.15	Figure 12

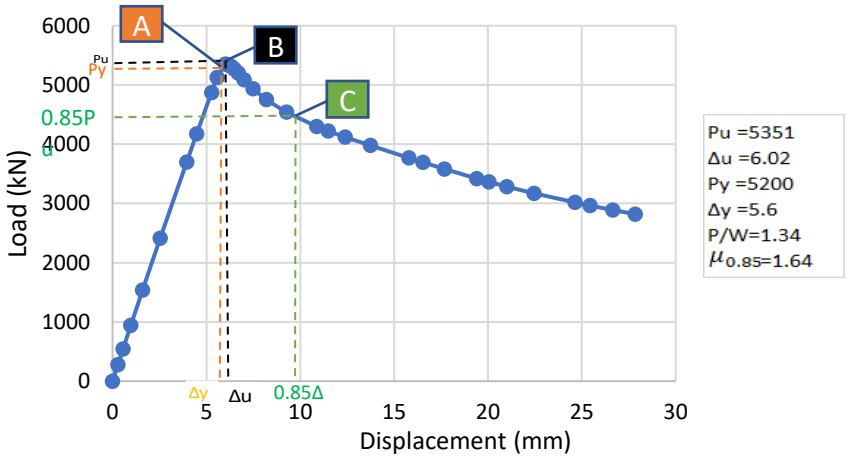

Figure 5: Failure status of the best performance short column with P/W=1.34

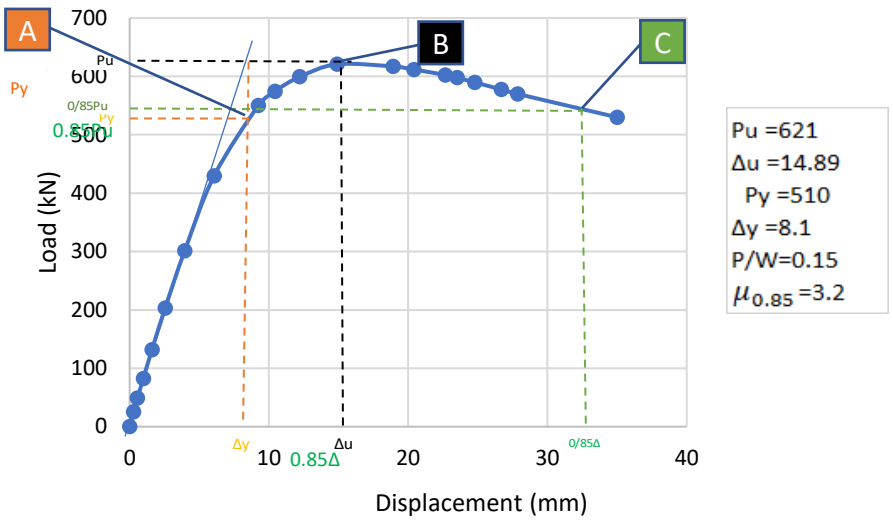

Figure 6: Failure status of the weakest performance short column with P/W=0.15

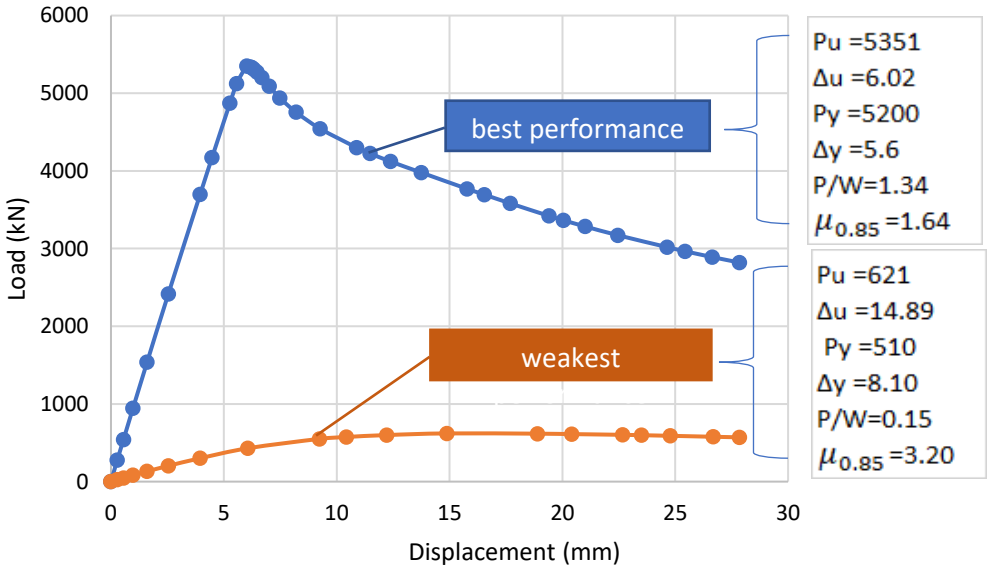

Figure 7: Performance comparison between the strongest and weakest short columns

4. Conclusions

In this manuscript, the L-shaped CFST columns with different eccentricities are studied. Numerical modeling is done using ABAQUS software to evaluate these columns under the effect of axial and off-axis loading. The changes in the eccentric bearing capacity of the studied columns are analyzed and compared based on the strength of steel and concrete. Also, the optimal performance of the examined columns is assessed according to the $\frac{P}{W}$ ratio (load-to-weight). The results of these analyzes are fully presented in the previous sections, and in this section the most important results are briefly stated:

- Under the effect of eccentric loading, the columns with thicknesses of 4, 6 and 8 mm do not have significant difference in the term of ductility. The biggest difference (equal to 7%) is observed in the eccentricity of 120 mm.
- The energy absorption of the column with tube thickness of 8 mm under loading with the eccentricity of -120 mm is 3.7 times more than the column with tube thickness of 4 mm and 1.7 times more than the column with tube thickness of 6 mm.
- In the comparison of the columns in terms of peak load under eccentric loading, the column with tube thickness of 8 mm has 74% and 25% more capacity than the column with tube thickness of 4 mm and the column with tube thickness of 6 mm (on average).

- Among the different parameters, the biggest impact on the eccentric bearing capacity of the columns is related to the thickness of the steel tube. Also, the least impact is related to the distance between connecting plate and the compressive strength of concrete.
- According to the acquired data, it is quite clear that the increase in height decreases the carrying capacity (i.e., reduction of $\frac{P}{W}$ ratio). The important point is that by simultaneously increasing the height of the column and its weight, reducing the thickness of the steel tube can optimize the columns performance of same rank (due to weight loss).
- For the column with a tube thickness of 8 mm, loading under e= −120 mm causes the greatest absorption of energy. For the column with a tube thickness of 6 mm, loading under e= −60 mm causes the greatest absorption of energy. For the column with a tube thickness of 4 mm, loading under e= 60 mm causes the greatest absorption of energy.

Conflict of interest

The authors declare that they have no any conflict of interest in this study.
The authors declare that they have no known competing financial interests or personal relationships that could have appeared to influence the work reported in this paper.
The authors declare the following financial interests/personal relationships which may be considered as potential competing interests:

Reference

Chen Z.H., Rang B., Apostolos F. (2009). "Axial compression stability of a crisscross section column composed of concrete-filled square steel tubes". *Journal of Mechanics of Materials and Structures*. 4, 1787-1799 https://doi.org/10.2140/jomms.2009.4.1787.

Chen Z., Liu J., Zhou T., Yan X., Zhang X. (2020). "Uniaxial eccentric-compression performance analysis for double-plate connected concrete-filled steel-tube composite columns". *Journal of Structural Engineering Archive*, 146(8), https://doi.org/10.1061/(ASCE)ST.1943-541X.0002700.

Chen X., Zhou T., Chen Z. Liu J., Jiang B. (2020). "Mechanical properties of special-shaped concrete filled steel tube columns under eccentric compression". *Journal of Constructional Steel Research*. 167, 105779 https://doi.org/10.1016/j.jcsr.2019.105779.

Dundar C., Tokgoz S., Tanrikulu A-K., Baran T., (2008). "Behaviour of reinforced and concrete-encased composite columns subjected to biaxial bending and axial load. Building and Environment". 43(6), 1109-1120, https://doi.org/10.1016/j.buildenv.2007.02.010.

Dancygier A.N ., Berkover E. (2016). "Cracking localization and reduced ductility in fiber-reinforced concrete beams with low reinforcement ratios. *Engineering Structures*", 111, 411-424.
https://doi.org/10.1016/j.engstruct.2015.11.046.

Ghandi E., Mohammadi R.N., Esmaeili Niari S., (2024). "Parametric Analysis of Axially Loaded Partially Concrete-Filled Cold-Formed Elliptical Columns Subjected to Lateral Impact Load". *Civil Engineering Infrastructures Journal*,
HTTPS://DOI.ORG/ 10.22059/CEIJ.2024.364758.1955

Hatzigeorgiou G.D., Beskos D.E., (2005). "Minimum cost design of fibre-reinforced concrete-filled steel tubular columns". *Journal of Constructional Steel Research*. 61(2), 167-182,
https://doi.org/10.1016/j.jcsr.2004.06.003

Labibzadeh M. Hashemi Tabatabaei S.M.J., Ghafouri H.R. (2018). "An efficient element free method for stress field assessment in 2D linear elastic cracked domains. Computational and Applied Mathematics", 37, 6719–6737,
https://doi.org/10.1007/s40314-018-0710-7

Labibzadeh M., Firouzi A., Ghafouri H-R., (2017). "Structural performance evaluation of an aged structure using a modified plasticity model in inverse solution method". *Inverse Problems in Science and Engineering*, 26(9), 1326-1355,
https://doi.org/10.1080/17415977.2017.1400028

Labibzadeh M., Hamidi R. (2017). "Effect of stress path, size and shape on the optimum parameters of a brittle-ductile concrete model". *Engineering Structures and Technologies*. 9(4), 195-206.

https://doi.org/10.3846/2029882X.2017.1414636
Ting Z., Zhexi Y., Zhihua C., Yue Y., (2024). "Seismic behavior of connections between H-beams and L-shaped column composed of concrete-filled steel tube mono-columns connected by double vertical plates". *Journal of Constructional Steel Research*, 198,
https://doi.org/10.1016/j.jcsr.2022.107513.
Tao Z., Han L.H., Wang D.Y. (2008). "Strength and ductility of stiffened thin-walled hollow steel structural stub columns filled with concrete". *Thin-Walled Structures*, 46(10), 1113-1128.
https://doi.org/10.1016/j.tws.2008.01.007
Wang Z., Ge L., Qingqing X., Haiwei G., (2023). "Seismic behavior of wide-limb special-shaped columns composed of concrete-filled steel tubes". *Journal of Constructional Steel Research*. 205.
https://doi.org/10.1016/j.jcsr.2023.107887.
Wang H.L., Xiong W., Yan L. G., Zi H. T., Jing Y. L., Wen H. B., (2024). "Experimental and numerical study of L-shaped irregularly concrete-filled steel tube columns under axial compression and eccentric compression". *Journal of Building Engineering*. 84,
https://doi.org/10.1016/j.jobe.2024.108572
Wang-H.L., Wen H.B., Yan L.G., Xiong W., (2024). "Design method of irregular-shaped concrete-filled steel tube column joints with inner semi-diaphragm". *Structures*. 60.
https://doi.org/10.1016/j.istruc.2024.105883.
Yang Y., Wang G., Yang W., Wei X., Frank-Chen Y. (2022). "Experimental research on fire behavior of L-shaped CFST columns under axial compression". *Journal of Constructional Steel Research*, 198, 107505.
https://doi.org/10.1016/j.jcsr.2022.107505
Zhang W., Chen Z., Xiong Q-Q. (2018). "Performance of L-shaped columns comprising concrete-filled steel tubes under axial compression". *Journal of Constructional Steel Research*, 145, 573-590.
https://doi.org/10.1016/j.jcsr.2018.03.007
Zhihua C., Mohammed A., Yansheng D., Mashrah W.A.H., Bingzhen ., Jin ., (204). "Experimental and numerical study on seismic performance of square and l-shaped Concrete-filled steel tubes column Frame-Buckling steel plate shear walls". *Engineering Structures*. 274.
https://doi.org/10.1016/j.engstruct.2022.115155.